Volume 60
Number 56
18 July 2024
Pages 7103–7234

ChemComm

Chemical Communications

rsc.li/chemcomm

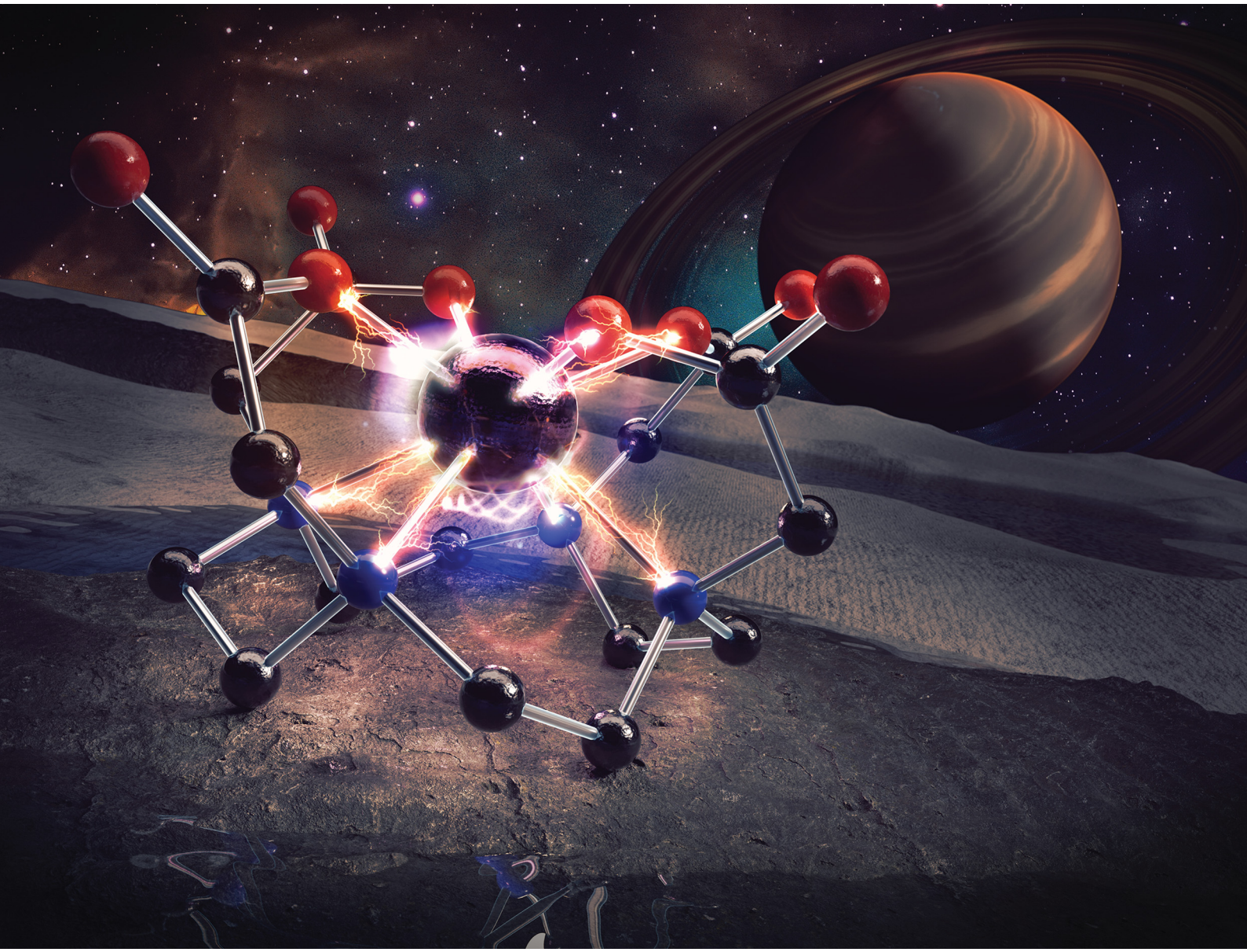

ISSN 1359-7345

ROYAL SOCIETY OF CHEMISTRY

COMMUNICATION

Tom C. H. Adamsen, Erwan Le Roux *et al.*
Synthesis and stability of the [^{45}Ti]Ti–DOTA complex: en route towards aza-macrocyclic ^{45}Ti-based radiopharmaceuticals

60 YEARS ANNIVERSARY

ChemComm

COMMUNICATION

View Article Online
View Journal | View Issue

Cite this: *Chem. Commun.*, 2024, **60**, 7148

Received 16th April 2024,
Accepted 3rd June 2024

DOI: 10.1039/d4cc01800a

rsc.li/chemcomm

Synthesis and stability of the [^{45}Ti]Ti–DOTA complex: en route towards aza-macrocyclic ^{45}Ti-based radiopharmaceuticals†‡

Tamal Roy, §[a] Eduard Pogorilyy, §[a] Chubina P. Kumarananthan,[b] Unni A. Kvitastein,[b] Marco Foscato,[a] Karl W. Törnroos,[a] Tom C. H. Adamsen *[ab] and Erwan Le Roux *[a]

We report the use of DOTA as a chelator for titanium. The resulting complex is fully characterised and *in vitro* stability studies reveal its high kinetic inertness against transmetallation and transchelation. The radiolabeling of DOTA with ^{45}Ti, *via* a guaiacol-based liquid–liquid extraction method, leads to a high radiochemical conversion up to 98%.

Titanium radionuclides were first synthesized over 80 years ago[2] and are currently being revived due to their promising characteristics in nuclear medicine, especially for positron emission tomography (PET) imaging.[3–7] From a cyclotron, two types of Ti isotopes can be produced: a long-lived titanium-44 (^{44}Ti: $t_{1/2}$ = 60 years)[8] which is not-well suited for direct PET applications, and titanium-45 (^{45}Ti: $t_{1/2}$ = 3.08 h, β^+: 84.8%, $E_{\beta+avg}$ = 439 keV)[3] with negligible secondary γ-emission (0.154%) and a low β^+ maximum endpoint energy of 1040.4 keV, which are favourable features for ensuring good image quality at low dosing for PET imaging.[6,7,9,10] With such a half-life, its distribution can also be facilitated by shipping it away from the cyclotron production site, in contrast to the commonly used radiopharmaceuticals with short-lived radionuclides such as ^{11}C ($t_{1/2}$ = 20.4 min), ^{18}F ($t_{1/2}$ = 109.7 min) and ^{68}Ga ($t_{1/2}$ = 67.6 min), for instance.[5,10] A further favourable aspect of ^{45}Ti is its low production cost as it can be obtained by irradiating naturally monoisotopic scandium *via* a ^{45}Sc(p,n)^{45}Ti transmutation reaction.[11]

However, owing to titanium's high oxophilicity, low hydrolytic stability, and high propensity in forming titanyl species in aqueous environments, the radiochemistry of ^{45}Ti currently remains underexploited.[7] The first labelled compounds of ^{45}Ti reported were based on [^{45}Ti]Ti–Cl_4 and [^{45}Ti]Ti–ascorbate. In 1982, Ishiwata reported a series of titanyl compounds made of [^{45}Ti]Ti–Cl_2(=O) and [^{45}Ti]Ti–phytate(=O) along with other chelators based on diethylenetriamine pentaacetic acid, citric acid and human serum albumin.[4,12] Recent reports also include mesoporous silica nanoparticles and proteins such as transferrin radiolabelled with ^{45}Ti, and employed as radiopharmaceutical vectors with a limited efficiency in tumour uptake.[13] Due to nonideal chelator–metal interactions, most of the *in-vivo* studies showed similar tissue biodistribution profiles of ^{45}Ti indicating that these Ti-complexes have low kinetic stability towards transchelation, and thus leading to poor radiotracer performances.[14] A handful of ^{45}Ti based radiometal involving acyclic chelators (open-chain) such as [^{45}Ti]Ti–salan, [^{45}Ti]Ti–DFO/LDFC and [[^{45}Ti]Ti–THP]$^+$ linked to various targeting vectors (bioconjugates such as PSMA and/or DUPA),[15–19] and without such as [[^{45}Ti]Ti–THP]$^+$ and [[^{45}Ti]Ti–TREN–CAM]$^{2-}$ were recently investigated.[20] While the "chelate effect" of these acyclic chelators has successfully led to a fast complexation, in most cases maximizing their thermodynamic and kinetic stabilities along with high radiolabelling, demetallation and degradation are still commonly observed to some extent under physiological conditions due to the intrinsic low kinetic inertness for this category of chelators.[7,17,18,21] To date, no attempts have been made to use macrocyclic chelators for titanium, specifically with aza-macrocycles such as the DOTA chelator, which is widely utilised in the radiopharmaceutical field,[22] and well-known for leading to more kinetically inert metal-complexes.[7,10,23] The main reason might be their alleged ineffectiveness in forming stable complexes with titanium, as quoted *ad verbum* "the cyclen family of popular chelators, such as 1,4,7,10-tetraazacyclododecane-1,4,7,10-tetraacetic acid (DOTA) and its derivatives, has not demonstrated any utility for chelating

[a] *Department of Chemistry, University of Bergen, Allégaten 41, Bergen, Norway. E-mail: Erwan.LeRoux@uib.no, Tom.Adamsen@uib.no*
[b] *Department of Radiology, Haukeland University Hospital, Centre for Nuclear Medicine and PET, Jonas Lies vei 65, Bergen, Norway*

† A data set collecting the results from the DFT modelling is available from the ioChem-BD repository and it can be accessed *via* **https://doi.org/10.19061/iochem-bd-6-344**, see ref. 1.

‡ Electronic supplementary information (ESI) available: Experimental section, DRIFT, 1–2D NMR and HR-MS spectra of M–DOTA complexes. Stability, DFT and ^{45}Ti-radiolabeling studies. See DOI: **https://doi.org/10.1039/d4cc01800a**

§ These authors contributed equally.

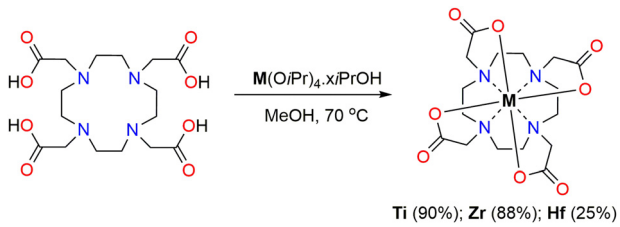

Scheme 1 Synthesis of M–DOTA complexes.

Ti^{4+}".[17] Contrary to the idea that DOTA and its derivatives are not suitable chelators for titanium, it remains very puzzling considering their recent successful application for zirconium-89.[7,9,24–26] Here, we report the synthesis of Ti–DOTA, its full characterization and stability, including against other competitive metals and the EDTA chelator. Additionally, we have successfully produced its corresponding radio-analogue, *i.e.*, [^{45}Ti]Ti–DOTA.

Non-radioactive Ti–DOTA can be obtained by stirring a mixture of DOTA in non-protic organic solvents or in methanol, followed by the addition of $Ti(OiPr)_4$ at 70 °C for 16 h (Scheme 1 and Table S1, ESI‡). In all cases, a white solid is obtained in relatively high yield (67–89%). An alternative starting precursor as $TiCl_4$ can also be used for forming Ti–DOTA in the presence of NEt_3 but leads to an inferior yield (27%) (Table S1, ESI‡).

Solid-state analysis of Ti–DOTA through diffuse reflectance infrared Fourier transform (DRIFT) spectroscopy indicates the disappearance of the broad ν(OH) stretching bands between 3200–2500 cm^{-1}, and ν(C=O) stretching band at 1744 cm^{-1} corresponding to the carboxylic acid groups, and the appearance of two $\nu_{as/s}(COO^-)$ stretching vibrations at 1679 and 1329 cm^{-1}, respectively. The difference of $\Delta\nu$ = 350 cm^{-1} between the ν_{as} and ν_s stretching bands is characteristic and consistent with the monodentate chelating mode (Fig. S1, ESI‡).[27] HR-MS analysis of this complex gives a $(M + H)^+$ signal at 449.1149 *m*/*z* with the highest abundance, which supports the formation of the Ti–DOTA complex (Fig. S2, ESI‡).

Given that the Ti–DOTA complex exhibits poor solubility in classical polar and non-polar solvents except water, which sparingly solubilizes this complex, the solution-state NMR spectroscopy was performed in D_2O. Owing to its C_4-symmetry, a well-resolved ^{1}H NMR spectrum was obtained, especially upon increasing the signal-to-noise ratio (NS = 128) without using a water suppression sequence (Fig. S3 (ESI‡) and Fig. 1). The ^{1}H NMR data show a spectral pattern comparable to Zr–DOTA (Fig. S9, ESI‡),[24,28] implying not only successful formation of the Ti–DOTA complex but also towards its structural similarity to Zr–DOTA. The assignments of the protons are further confirmed using 2D ^{1}H–^{1}H correlation (COSY, NOESY) and ^{1}H–^{13}C correlation (HSQC, HMBC) spectra, and the results agree with the presence of only one type of major conformer in solution (Fig. 1 and Fig. S4–S6, ESI‡), *i.e.*, belonging either to a square antiprism (SAP) or twisted square antiprism (TSAP), including their enantiomers $\Delta(\lambda\lambda\lambda\lambda)/\Lambda(\delta\delta\delta\delta)$ and $\Lambda(\lambda\lambda\lambda\lambda)/\Delta(\delta\delta\delta\delta)$, respectively, as reported for other M–DOTA (M = Ln, Zr, Tl, Bi).[25,28–31] A complete major conformer determination, as previously established for Ln–DOTA complexes[29]

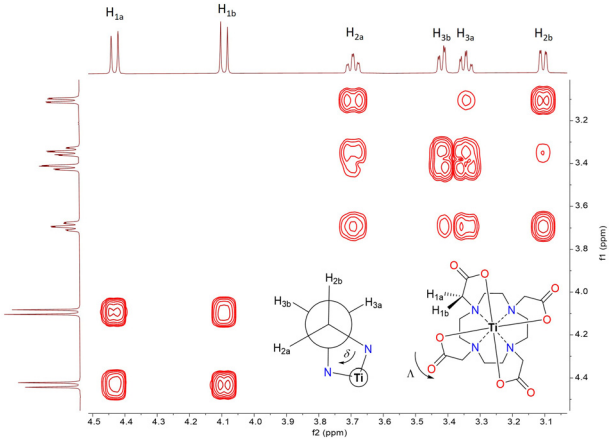

Fig. 1 2D ^{1}H–^{1}H COSY spectrum of Ti–DOTA in D_2O.

by mean of variable temperature NMR experiments, was not possible due to the limited solubility of this Ti-complex. The ^{13}C NMR spectrum of Ti–DOTA shows characteristic chemical resonances at δ 180.1 (–O*C*O), 69.7 (–*C*H_2–COO) and 59.3/58.2 (–*C*H_2*C*H_2–) ppm (Fig. S7, ESI‡) with narrow line widths corroborating the presence of only one conformer in solution, unless the exchange rate between the two conformers SAP ↔ TSAP is very fast at the NMR timescale.

Ti–DOTA crystallizes in aqueous solution as long colourless needles, but the obtained crystals were ill-suitable for single X-ray diffraction due to consistent merohedral rotational twinning. Nevertheless, we recorded Powder X-ray Diffraction (PXRD) for the synthesized Ti–DOTA complex, and the pattern was compared with the patterns of rutile, anatase and brookite to eliminate any doubt of the presence of crystalline TiO_2 in addition to Ti–DOTA in the solid-state (Fig. S8, ESI‡). To gain further insight into the structural aspect of Ti–DOTA, we synthesized Hf–DOTA and the previously reported Zr–DOTA[24] under identical reaction conditions (Scheme 1). HR-MS analyses indicate the formation of both Zr- and Hf–DOTA with the base peak at 491.0712 and 581.1136 *m*/*z*, respectively (Fig. S9 and S16, ESI‡). Both Zr- and Hf–DOTA displayed similar patterns in ^{1}H, ^{13}C and 2D NMR and DRIFT spectra like for Ti–DOTA (Fig. S1, S10–S15 and S17–S22, ESI‡), which essentially indicates that all three complexes have similar structural aspects in solution and in the solid-state. Similarly to Ti–DOTA, crystals of limited quality, yet again merohedrally twinned, of Hf–DOTA were obtained from an aqueous solution at room temperature, but in this case allowing deduction of the connectivity around the Hf-centre (Fig. S23, ESI‡). Hf–DOTA crystallizes as two overlapping 8-coordinate enantiomers, namely $\Delta(\lambda\lambda\lambda\lambda)$ and $\Lambda(\delta\delta\delta\delta)$, in which both exhibit an SAP geometry identical to Zr–DOTA.[24]

To gather further insights into the structural aspects and relative stabilities of the M–DOTA complexes (M = Ti, Zr, Hf), we opted for DFT studies of these complexes (PBE-GD3MBJ-SMD(water)/def2-TZVP/D, see ESI‡). The crystallographic structure reported for Zr–DOTA shows a co-crystallized enantiomeric pair of κ^8 conformations $\Lambda(\delta\delta\delta\delta)$ and $\Delta(\lambda\lambda\lambda\lambda)$, *i.e.*, only as SAP

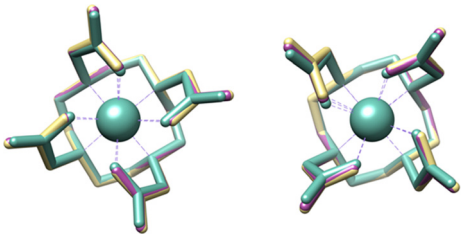

Fig. 2 DFT-optimized geometries of Ti–DOTA (green), Zr–DOTA (gold), and Hf–DOTA (purple) in the SAP/Λ(δδδδ) (left) and TSAP/Δ(δδδδ) (right) configuration.

conformers.[24] Notably, DOTA can also coordinate metals in κ^8 chelation mode with the diastereomeric conformations leading to complexes Δ(δδδδ) and Λ(λλλλ) as experimentally shown by the crystal structure of the [Bi–DOTA]$^-$ complex where the geometry around Bi adopts a TSAP.[30] Both geometries were modelled with DFT for Ti(IV), Zr(IV), and Hf(IV), but Λ(δδδδ) is found to be more stable than Δ(δδδδ) by 4–5 kcal mol^{-1} for all three metals (Fig. S24, S25 and Table S2, ESI‡), which is consistent with the geometry observed in the crystal structures of Zr–DOTA.[24] Notably, while the Λ(δδδδ) M–DOTA geometries of the three metals are all similar (Fig. 2), the Ti complexes appear slightly more compact than the Zr and Hf analogues. In fact, the M–O distances in the DFT-modelled structures are 2.03–2.04 Å in Ti–DOTA and 2.17–2.20 Å in Zr–DOTA. Instead, the Ti–N distances are 2.39 Å and the Zr–N distances are 2.47–2.49 Å. Overall, these distances show that the κ^8-metal-coordinating environment of Ti–DOTA is more compact than those of Zr–DOTA and Hf–DOTA (M–N_4/M–O_4 distances: Ti: 1.278/0.977 Å; Zr: 1.382/0.915 Å and Hf: 1.351/0.937 Å, Table S3, ESI‡). The index parameters (τ_8), indicating the degree of idealised SAP (τ_8 = 0) and TSAP (τ_8 = 1) geometries (Table S3, ESI‡), for the non-capped 8-coordinate Zr–DOTA complexes determined from the X-ray structures and obtained from DFT are also in line with an SAP geometry with τ_8 of 0.17 and 0.14/0.15, respectively. Furthermore, Ti–DOTA with its calculated τ_8 of 0.07 is the lowest of all known M–DOTA complexes, indicating that the Ti centre adopts a nearly ideal SAP geometry, and thus is somehow shift-locked within the M–DOTA structure compared to Zr and Hf atoms or other larger metal atoms.

Next, we evaluate the *in vitro* stability of the Ti–DOTA complex due to the perceived idea of aza-macrocycles being labile chelates for titanium ions. Accordingly, the kinetic stability of Ti–DOTA was studied at physiological pH (7.4) and temperature (37 °C) in the presence of competitive metal ions (Mg^{2+}, Fe^{3+}, Co^{2+}, Cu^{2+} and Zn^{2+}) as well as with an excess of EDTA chelator. Under these conditions, Ti–DOTA was found to be highly kinetically inert against transmetallation and DOTA dissociation (Table S4, ESI‡). The thermodynamic stability of the M–DOTA complexes was also assessed by DFT studies using two different methods. We first considered the free energy of complexation of the metal-aquo cation $[M(H_2O)_{19}]^{4+}$ (M = Ti, Zr, Hf) by the anionic free DOTA^{4-}, similarly to previous work in the field.[32] The resulting thermodynamic preference for the complex is much higher for Ti than for Zr and Hf (Table S5, ESI‡). Notably, the Hf complex is predicted to be more stable than the Zr analogue, but overall, this trend correlates well with the effective ionic radii for 8-coordinate compounds: Ti(IV) = 0.74 Å, Zr(IV) = 0.84 Å, Hf(IV) = 0.83 Å.[33] This trend is also confirmed by the estimation of the free energy for the exchange of EDTA^{4-} with DOTA^{4-} (Table S5, ESI‡). The Ti–DOTA complex is confirmed to be the most stable in the series, and significantly separated from Hf, *i.e.*, the second most stable, and Zr.

The salt-based liquid target production of ^{45}Ti was performed using $^{nat}Sc(NO_3)_3$ dissolved in ultrapure HNO_3 and irradiated with a proton beam current of 10–25 μA for 1.5–3 h (Table S6, ESI‡). The irradiations resulted in a ^{45}Ti-activity at the end of bombardment (EOB) ranging from 0.31 to 1.25 GBq with an average radionuclidic purity of 98.0% (Table S6, ESI‡).

Initial attempts were made to separate [^{45}Ti]Ti-HNO_3 from the scandium matrix using a cation-exchange hydroxamate-modified resin (ZR-resin) as previously reported (Scheme S1, ESI‡).[11] An extraction efficiency (EE) of only *ca.* 5% was achieved during the solid-phase extraction with the ZR-resin using 1 M oxalic acid as an eluent. Most importantly, no subsequent ligand exchange with the presumed [^{45}Ti]Ti–oxalate species was identified in the presence of DOTA by radio-HPLC/HPLC with Ti–DOTA as a reference. Trying to remediate this drawback, a ligand exchange was attempted through a QMA anion exchange resin as successfully reported for the conversion of [^{89}Zr]Zr–$(Ox)_2$ to [^{89}Zr]Zr–DOTA in high yield *via* a more reactive intermediate [^{89}Zr]Zr–Cl_4.[24,34] In our case, the ligand exchange with QMA-resin did not proceed as for its Zr analogue (Scheme S1, ESI‡), presumably due to the high stability of [^{45}Ti]Ti–oxalate species in aqueous media.[35] Other eluants such as 0.1/1 M citric acid, and 1 M ascorbic acid were also tested but resulted in poor extraction efficiency <6%, and subsequent formation of [^{45}Ti]Ti–DOTA was not observed by reacting the eluates with DOTA. These results indicate the slow kinetic formation of Ti–DOTA, contrasting the rapid complex formation with acyclic chelators such as DFO/LDFC, TREN–CAM^{2-} and THP, where the ^{45}Ti radiolabelling is straightforwardly obtained *via* the intermediate [^{45}Ti]Ti–citrate, for instance.[18–20] To mimic the reactivity of Ti–oxalate species with DOTA, we attempted to form a non-radioactive Ti–DOTA complex by refluxing DOTA with bis(ammonium lactato)dihydroxide titanium for 24 h in water. Only a 2% yield was achieved, indicating a remarkable stability of such derived Ti–oxalate species (Table S1, ESI‡).[35] Alternatively, a liquid–liquid extraction (LLE) method was carried out for purifying ^{45}Ti from its $^{nat}Sc(NO_3)_3$ liquid matrix, hence avoiding strongly binding chelators and for replacing them by a more labile chelator such as guaiacol.[36] Following the procedure reported by Zhuravlev,[16,17] a mixture of guaiacol and anisole (9/1 v/v) was used for the separation of Sc from [^{45}Ti]Ti–HNO_3 (Scheme S2, ESI‡). With an optimized ratio of 1 : 1.3 (aqueous/organic phase) (v/v), an extraction efficiency of 81% (d.c.) was obtained comparable to the range of EEs (75–85%) obtained by LLE protocols in continuous flow using a membrane separator module.[17] The radiolabelling of DOTA was achieved by mixing the organic phase solution containing 93.6 MBq

(2.53 mCi) of [^{45}Ti]Ti–guaiacolate with a solution of DOTA (50 mM) in DMSO in the presence of an excess of pyridine. The reaction mixture was incubated at 60 °C for 15 min and a radiochemical conversion of 98% was determined (Fig. S26 and S27, ESI‡). Subsequently, the complex was purified using preparative radio-HPLC to obtain 15% RCY (d.c.) of the pure [^{45}Ti]Ti–DOTA complex (Fig. S28, ESI‡).

In summary, we now report the first example of a DOTA complex of titanium, contradicting the established opinion that aza-macrocycles such as DOTA are not suitable chelators for Ti^{4+} ions. To the contrary, our DFT studies show a remarkable stability of the Ti–DOTA complex, even superior to their Zr and Hf analogues and supported experimentally by *in vitro* stability studies. In addition, our preliminary results on the radiolabelling of DOTA demonstrate that [^{45}Ti]Ti–DOTA can be efficiently obtained *via* a LLE method. Albeit the radiolabelling with ^{45}Ti isotope was hitherto limited to acyclic chelators, this example using an aza-macrocyclic chelator opens new opportunities for ^{45}Ti-based radiopharmaceutical development applied to PET imaging.

This work was supported by the Trond Mohn Foundation, project no. TMS2019TMT07 and the University of Bergen. The Research Council of Norway is thanked for CPU (NN2506K) and storage resources (NS2506K). We would like to acknowledge the Haukeland University Hospital cyclotron team for enabling the production of ^{45}Ti, and C. Bruhn for QMA-resin experiments. Prof. Dr N. Å. Frøystein and Dr D. Kratzert are thanked for their fruitful discussions on NMR spectroscopy and on crystallographic issues, respectively.

Conflicts of interest

There are no conflicts to declare.

Notes and references

1 M. Álvarez-Moreno, C. de Graaf, N. López, F. Maseras, J. M. Poblet and C. Bo, *J. Chem. Inf. Model.*, 2015, **55**, 95–103.
2 J. S. V. Allen, M. L. Pool, J. D. Kurbatov and L. L. Quill, *Phys. Rev.*, 1941, **60**, 425–429; C. Ishii and K. Takahashi, *J. Phys. Soc. Jpn.*, 1960, **15**, 736–737; D. Gföller and A. Flammersfeld, *Z. Phys.*, 1965, **187**, 490–494; F. T. Porter, M. S. Freedman, F. Wagner and K. A. Orlandini, *Phys. Rev.*, 1966, **146**, 774–780; W. M. Zuk, W. F. Davidson, M. R. Najam and M. A. Awal, *Z. Phys.*, 1971, **242**, 93–101.
3 J. C. Merrill, R. M. Lambrecht and A. P. Wolf, *Int. J. Appl. Radiat. Isot.*, 1978, **29**, 115–116.
4 K. Ishiwata, T. Ido, M. Monma, M. Murakami, M. Kameyama, H. Fukuda and T. Matsuzawa, *J. Labelled Compd. Radiopharm.*, 1982, **19**, 539–1541.
5 A. L. Vāvere, R. Laforest and M. J. Welch, *Nucl. Med. Biol.*, 2005, **32**, 117–122.
6 P. Costa, L. F. Metello, F. Alves and M. Duarte Naia, *Instruments*, 2018, **2**, 8.
7 E. Boros and A. B. Packard, *Chem. Rev.*, 2019, **119**, 870–901.
8 T. Hashimoto, K. Nakai, Y. Wakasaya, I. Tanihata, Z. Fulop, H. Kumagai, A. Ozawa, K. Yoshida and R. Goswarmi, *Nucl. Phys. A*, 2001, **686**, 591–599.
9 M. Brandt, J. Cardinale, M. L. Aulsebrook, G. Gasser and T. L. Mindt, *J. Nucl. Med.*, 2018, **59**, 1500.
10 T. I. Kostelnik and C. Orvig, *Chem. Rev.*, 2019, **119**, 902–956.
11 I. F. Chaple, K. Thiele, G. Thaggard, S. Fernandez, E. Boros and S. E. Lapi, *Appl. Radiat. Isot.*, 2020, **166**, 109398.
12 M. Kawamura, K. Inoue, S. Kimura, T. Ido, K. Ishiwata, K. Kawashima, K. Matsuda and M. Kameyama, *J. Labelled Compd. Radiopharm.*, 1986, **23**, 1360–1362; K. Ishiwata, T. Ido, M. Monma, M. Murakami, H. Fukuda, M. Kameyama, K. Yamada, S. Endo, S. Yoshioka, T. Sato and T. Matsuzawa, *Int. J. Radiat. Appl. Instrum. Part A. Appl. Radiat. Isot.*, 1991, **42**, 707–712.
13 A. L. Vavere and M. J. Welch, *J. Nucl. Med.*, 2005, **46**, 683–690; F. Chen, H. F. Valdovinos, R. Hernandez, S. Goel, T. E. Barnhart and W. Cai, *Acta Pharmacol. Sin.*, 2017, **38**, 907–913.
14 S. Saini and S. E. Lapi, *Pharmaceuticals*, 2024, **17**, 479.
15 G. W. Severin, C. H. Nielsen, A. I. Jensen, J. Fonslet, A. Kjær and F. Zhuravlev, *J. Med. Chem.*, 2015, **58**, 7591–7595; K. Giesen, I. Spahn and B. Neumaier, *J. Radioanal. Nucl. Chem.*, 2020, **326**, 1281–1287.
16 K. S. Pedersen, J. Imbrogno, J. Fonslet, M. Lusardi, K. F. Jensen and F. Zhuravlev, *React. Chem. Eng.*, 2018, **3**, 898–904.
17 S. K. Pedersen, C. Baun, M. K. Nielsen, H. Thisgaard, I. A. Jensen and F. Zhuravlev, *Molecules*, 2020, **25**, 1104.
18 I. F. Chaple, H. A. Houson, A. Koller, A. Pandey, E. Boros and S. E. Lapi, *Nucl. Med. Biol.*, 2022, **108–109**, 16–23.
19 S. Saini, G. E. D. Mullen, P. J. Blower and S. E. Lapi, *Mol. Pharmaceutics*, 2024, **21**, 822–830.
20 A. J. Koller, S. Saini, I. F. Chaple, M. A. Joaqui-Joaqui, B. M. Paterson, M. T. Ma, P. J. Blower, V. C. Pierre, J. R. Robinson, S. E. Lapi and E. Boros, *Angew. Chem., Int. Ed.*, 2022, **61**, e202201211; A. J. Koller, L. Wang, M. Deluca, O. Glaser, M. J. Robis, J. C. Mixdorf, M. N. Chernysheva, I. A. Guzei, E. Aluicio-Sarduy, T. E. Barnhart, J. W. Engle and E. Boros, *Inorg. Chem.*, 2023, **62**, 20655–20665.
21 R. Lengacher, A. Marlin, D. Śmiłowicz and E. Boros, *Chem. Soc. Rev.*, 2022, **51**, 7715–7731.
22 N. Herrero Álvarez, D. Bauer, J. Hernández-Gil and J. S. Lewis, *ChemMedChem*, 2021, **16**, 2909–2941.
23 J. J. R. Frausto da Silva, *J. Chem. Educ.*, 1983, **60**, 390; R. D. Hancock, *Pure Appl. Chem.*, 1986, **58**, 1445–1452; R. D. Hancock, *J. Chem. Educ.*, 1992, **69**, 615–621; N. Viola-Villegas and R. P. Doyle, *Coord. Chem. Rev.*, 2009, **253**, 1906–1925; Z. Baranyai, G. Tircsó and F. Rösch, *Eur. J. Inorg. Chem.*, 2020, 36–56.
24 D. N. Pandya, N. Bhatt, H. Yuan, C. S. Day, B. M. Ehrmann, M. Wright, U. Bierbach and T. J. Wadas, *Chem. Sci.*, 2017, **8**, 2309–2314.
25 D. N. Pandya, K. E. Henry, C. S. Day, S. A. Graves, V. L. Nagle, T. R. Dilling, A. Sinha, B. M. Ehrmann, N. B. Bhatt, Y. Menda, J. S. Lewis and T. J. Wadas, *Inorg. Chem.*, 2020, **59**, 17473–17487.
26 J. K. Yoon, B. N. Park, E. K. Ryu, Y. S. An and S. J. Lee, *Int. J. Mol. Sci.*, 2020, **21**, 4309.
27 C. C. R. Sutton, G. da Silva and G. V. Franks, *Chem. – Eur. J.*, 2015, **21**, 6801–6805.
28 D. Parker, K. Pulukkody, F. C. Smith, A. Batsanov and J. A. K. Howard, *J. Chem. Soc., Dalton Trans.*, 1994, 689–693.
29 S. Aime, M. Botta and G. Ermondi, *Inorg. Chem.*, 1992, **31**, 4291–4299.
30 É. Csajbók, Z. Baranyai, I. Bányai, E. Brücher, R. Király, A. Müller-Fahrnow, J. Platzek, B. Radüchel and M. Schäfer, *Inorg. Chem.*, 2003, **42**, 2342–2349.
31 C. Chen, C. Sommer, H. Thisgaard, V. McKee and C. J. McKenzie, *RSC Adv.*, 2022, **12**, 5772–5781.
32 J. P. Holland, *Inorg. Chem.*, 2020, **59**, 2070–2082.
33 R. Shannon, *Acta Cryst.*, 1976, **A32**, 751–767.
34 J. P. Holland, Y. Sheh and J. S. Lewis, *Nucl. Med. Biol.*, 2009, **36**, 729–739.
35 G. M. H. Van de Velde, *J. Inorg. Nucl. Chem.*, 1977, **39**, 1357–1362; P. Chaudhuri and H. Diebler, *J. Chem. Soc., Dalton Trans.*, 1977, 596–601.
36 P. Sobota, K. Przybylak, J. Utko, L. B. Jerzykiewicz, A. J. L. Pombeiro, M. F. C. Guedes da Silva and K. Szczegot, *Chem. – Eur. J.*, 2001, **7**, 951–958.